



Published in final edited form as:

Lab Invest. 2010 October ; 90(10): 1457–1467. doi:10.1038/labinvest.2010.107.

## Intestinal FXR-mediated FGF15 production contributes to diurnal control of hepatic bile acid synthesis in mice

Johanna HM Stroeve<sup>1</sup>, Gemma Brufau<sup>1</sup>, Frans Stellaard<sup>2</sup>, Frank J Gonzalez<sup>3</sup>, Bart Staels<sup>4,5,6</sup>, and Folkert Kuipers<sup>1,2</sup>

<sup>1</sup>Department of Pediatrics, Center for Liver, Digestive and Metabolic Diseases, University Medical Center Groningen, University of Groningen, Groningen, The Netherlands <sup>2</sup>Department of Laboratory Medicine, Center for Liver, Digestive and Metabolic Diseases, University Medical Center Groningen, University of Groningen, Groningen, The Netherlands <sup>3</sup>Laboratory of Metabolism, Center for Cancer Research, National Cancer Institute, National Institutes of Health, Bethesda, MD, USA <sup>4</sup>Département d'Athérosclérose, Institut Pasteur de Lille, Lille, France <sup>5</sup>INSERM UMR 545, Lille, France <sup>6</sup>Faculté des Sciences Pharmaceutiques et Biologiques et Faculté de Médecine, Université de Lille 2, Lille, France

### Abstract

Hepatic bile acid synthesis is subject to complex modes of transcriptional control, in which the bile acid-activated nuclear receptor farnesoid X receptor (FXR) in liver and intestine-derived, FXR-controlled fibroblast growth factor 15 (Fgf15) are involved. The Fgf15 pathway is assumed to contribute significantly to control of hepatic bile acid synthesis. However, scientific evidence supporting this assumption is primarily based on gene expression data. Using intestine-selective FXR knockout mice (iFXR-KO), we show that contribution of intestinal FXR-Fgf15 signalling in regulation of hepatic cholesterol 7 $\alpha$ -hydroxylase (*Cyp7A1*) expression depends on time of the day with increased hepatic *Cyp7A1* expression in iFXR-KO mice compared with controls exclusively during the dark phase. To assess the physiological relevance hereof, we determined effects of intestine-selective deletion of FXR on physiological parameters such as bile formation and kinetics of the enterohepatic circulation of bile acids. It appeared that intestinal FXR deficiency leads to a modest but significant increase in cholic acid pool size, without changes in fractional turnover rate. As a consequence, bile flow and biliary bile acid secretion rates were increased in iFXR-KO mice compared with controls. Feeding a bile acid-containing diet or treatment with a bile acid sequestrant similarly affected bile formation in iFXR-KO and control mice and induced similar changes in *Cyp7A1* and *Cyp8B1* expression patterns. In conclusion, this study is the first to demonstrate the physiological relevance of the contribution of the intestinal FXR-Fgf15 signalling pathway in control of hepatic bile acid synthesis. Fgf15 contributes to the regulation of hepatic bile acid synthesis in mice mainly during the dark phase. Expansion of the circulating bile

Correspondence: JHM Stroeve, MSc, Department of Pediatrics, Center for Liver, Digestive and Metabolic Diseases, CMC V, University Medical Center Groningen, Hanzplein 1, PO Box 30.001, Groningen 9700 RB, The Netherlands. J.H.M.Stroeve@med.umcg.nl.

#### DISCLOSURE/CONFLICT OF INTEREST

The authors declare no conflict of interest.

Supplementary Information accompanies the paper on the Laboratory Investigation website (<http://www.laboratoryinvestigation.org>)

acid pool as well as bile acid sequestration diminishes the contribution of intestinal FXR-Fgf15 signalling in control of hepatic bile acid synthesis and bile formation.

### Keywords

bile acids; circadian rhythm; Cyp7A1; enterohepatic circulation; Fgf15; Fxr

Bile acids are synthesized from cholesterol in the liver by at least two well-characterized synthetic cascades, ie, the 'classical' neutral pathway and the 'alternative' acidic pathway.<sup>1</sup> Bile acids serve a variety of important physiological functions in the body. One of the prominent functions of bile acids is in the generation of bile formation in the liver: the biliary pathway is a major route for removal of endo- and xenobiotics as well as of excess cholesterol.<sup>1</sup> Under fasting conditions, bile is stored in the gallbladder. Upon ingestion of a meal, bile is released from the gallbladder and secreted into the intestinal lumen, where bile acids facilitate the digestion and absorption of dietary lipids and fat-soluble vitamins.<sup>1</sup> Approximately 95% of the total bile acid pool will be reabsorbed by specific transporters present in the terminal ileum and transported back to the liver for resecretion into bile, thereby completing the so-called enterohepatic circulation. In this way, a pool of bile acids is maintained that ensures optimal concentrations of these natural detergents at their sites of action. Non-absorbed bile acids (5%) will enter the colon and are either, after being converted into secondary bile acids by bacteria, passively absorbed to enter the pool or disposed from the body through the feces. To compensate for this fecal loss, the liver will synthesize bile acids from cholesterol to maintain bile acid pool size.<sup>1</sup> Apart from their well-known functions in bile formation, cholesterol homeostasis and fat absorption, bile acids are now also known to exert regulatory roles in triglyceride and glucose metabolism.<sup>1</sup> Hence, tight control of bile acid pool size, composition and cycling frequency is of physiological relevance.

During the past years, it has become clear that the farnesoid X receptor (FXR, also known as NR1H4), a bile acid-sensing nuclear receptor, has a key function in the maintenance of bile acid homeostasis.<sup>2-4</sup> FXR is involved in control of bile acid synthesis in the liver and of bile acid transport through the enterohepatic circulation. This nuclear receptor is expressed in the liver and intestine as well as in other organs and tissues such as adrenals and adipose tissue.<sup>5,6</sup> Upon its activation, hepatic FXR suppresses bile acid synthesis by transcriptional downregulation of Cyp7A1,<sup>7,8</sup> the enzyme that catalyzes the first and rate-controlling step in the primary bile acid synthesis cascade. A previous study from our laboratory has demonstrated that FXR-null mice show, as expected, increased hepatic *Cyp7A1* gene expression levels. Furthermore, these mice turned out to have an increased cholic acid synthesis rate and an expanded cholic acid pool size.<sup>3</sup>

However, apart from the inhibitory actions of activated hepatic FXR, *Cyp7A1* is regulated through several other FXR-dependent and -independent mechanisms. Several CLOCK-dependent transcription factors are involved in the maintenance of the circadian expression of *Cyp7A1*, ie, Dbp, Rev-erba and E4BP4.<sup>9-11</sup> In addition, an intriguing mode of FXR-mediated control on hepatic *Cyp7A1* expression is exerted by indirect signalling from the

small intestine. Bile acid-induced activation of intestinal FXR induces expression of murine fibroblast growth factor 15 (*Fgf15*)<sup>12</sup> and of its human orthologue FGF19.<sup>13</sup> In contrast to most other Fgf proteins, Fgf15/19 has a weak heparin-binding affinity, which enables it to escape from being captured in extracellular matrices. As a consequence, intestine-derived Fgf15 is able to reach the liver and act as an endocrine factor.<sup>14</sup> Upon activation of its hepatic receptor, Fgf receptor isotype 4 (FGFR4), which requires  $\beta$ Klotho as a co-receptor for optimal functionality, *Cyp7A1* expression is repressed.<sup>14,15</sup>

Kim *et al*<sup>16</sup> recently compared bile acid metabolism in liver- and intestine-specific FXR knockout mice to examine the relative contributions of hepatic and intestinal FXR in control of hepatic bile acid synthesis. However, the conclusions of Kim *et al*<sup>16</sup> are merely based on rather moderate differences at the gene expression level. In this study, we address the relative contribution of the FXR-Fgf15 pathway to hepatic bile acid synthesis not only by examining changes at the gene expression level but, more importantly, also by determining the effect of intestine-selective deletion of FXR on physiological parameters such as bile formation and kinetics of the enterohepatic circulation of bile acids. In addition, the relative contribution of the intestinal FXR-Fgf15 signalling pathway is determined during the modulation of the bile acid pool by bile acid feeding and bile acid sequestration. Fgf15 contributes to the regulation of hepatic bile acid synthesis in mice mainly during the dark phase. Expansion of the circulating bile acid pool and bile acid sequestration diminishes the contribution of intestinal FXR-Fgf15 signalling in control of hepatic bile acid synthesis and bile formation.

## MATERIALS AND METHODS

### Animals

The intestine-selective FXR knockout mice were generated by cross-breeding of mice with loxP sites flanking the last FXR exon, containing the ligand-binding domain (described by Sinal *et al*<sup>4</sup>), with mice harboring cre-recombinase under the control of the villin promoter (Villin-Cre mice<sup>17</sup>). Animals were maintained on a C57B/6;129 mixed background.

Animals used in this study, male and female homozygous knockout mice (iFXR-KO) and wild-type (WT) littermates, were housed in a light- and temperature-controlled facility and received standard laboratory chow (RMH-B, Abdiets, Woerden, The Netherlands) and water *ad libitum*. When indicated, the endogenous FXR ligand TCA or the bile acid sequestrant Colesevelam HCl were mixed with the standard laboratory chow. The mice received humane care, and experimental procedures were in accordance with the local guidelines for use of experimental animals.

### Materials

[2,2,4,4-<sup>2</sup>H]-cholate ([<sup>2</sup>H<sub>4</sub>]-cholate, isotopic purity 98%) was obtained from Isotec (Miamisburg, OH, USA), and Colesevelam HCl was kindly provided by Daiichi Sankyo (Parsippany, NJ, USA).

## Experimental Procedures

In the first three experiments, mice were fed normal laboratory chow. The patterns of FXR and Fgf15 expression along the small intestine were examined in fed male WT and iFXR-KO mice ( $N = 3$ ), killed in the morning (0900 hours). The small intestine was rinsed with phosphate-buffered saline (PBS) and divided into six parts: 0, 33, 66, 83, 90 and 100% (relative distance from the stomach to distal ileum). Intestinal segments were frozen in liquid nitrogen and stored at  $-80^{\circ}\text{C}$  until RNA isolation.

Subsequently, the circadian rhythms of genes involved in hepatic bile acid synthesis were determined in 6–7 female WT and iFXR-KO mice. At 0700, 1300, 1900 and 0100 hours, mice were killed in the fed condition and the livers and terminal ilea were excised, (snap-)frozen and stored at  $-80^{\circ}\text{C}$  until RNA isolation. mRNA expression levels were analyzed by means of real-time quantitative PCR (see below).

Under isoflurane anesthesia, 300  $\mu\text{g}$  of [ $^2\text{H}_4$ ]-cholate in a solution of 0.1%  $\text{NaHCO}_3$  in PBS ( $\text{pH} = 7.4$ ) was intravenously administered to male WT and iFXR-KO mice ( $N = 6$ ). Every 12 h ( $t = 12$  till  $t = 60$ ) a retro-orbital blood sample of about 75  $\mu\text{l}$  was taken. Plasma was obtained by means of centrifugation (4000 r.p.m., 10 min,  $4^{\circ}\text{C}$ ). At  $t = 60$  h, the mice were anesthetized with a mixture of hypnorm (1 ml/kg) and diazepam (10 mg/kg) and subjected during 30 min to bile duct cannulation for the collection of bile.<sup>18</sup> During this collection period, the animals were placed in a humidified incubator to ensure maintenance of body temperature. Subsequently, mice were killed by cardiac puncture and the livers, distal small intestines and terminal ilea were excised. Livers and small intestinal segments were (snap-)frozen in liquid nitrogen and stored at  $-80^{\circ}\text{C}$  until RNA isolation and biochemical analysis. Feces and urine were collected from individual mice.

To evaluate the effects of supplementing/sequestering FXR ligands, male WT and iFXR-KO mice ( $N = 5$ ) were either fed during 3 days the normal laboratory chow enriched with 0.5% taurocholic acid (TCA) or were fed for 7 days normal chow enriched with 2% Colesevelam HCl. At the end of these periods, the mice were subjected to bile duct cannulation.<sup>18</sup> Mice were killed by means of cardiac puncture and the livers, distal small intestines and terminal ilea were excised and (snap-)frozen and stored at  $-80^{\circ}\text{C}$  until RNA isolation and biochemical analysis. Feces were collected from individual mice.

## Analytical Procedures

Livers were homogenized in ice-cold saline. Hepatic and biliary lipids were extracted according to Bligh and Dyer.<sup>19</sup> Commercially available kits (total and unesterified cholesterol, unesterified-free fatty acids and phospholipids (Wako, Neuss, Germany) and triglycerides (Roche, Mannheim, Germany)) were used to determine the lipid profiles in plasma, bile and liver. Bile salt concentrations in plasma, bile and feces were determined by an enzymatic fluorimetric assay.<sup>20</sup> Plasma AST and ALT levels were determined by routine clinical-chemical procedures on a P800 unit of a modular analytics serum work area from Roche Diagnostics (Basel, Switzerland). Histological examination of liver morphology was assessed by hematoxylin/eosin staining of formalin-fixed material by standard procedures.

## Steady-State mRNA Levels Determined by Real-Time Quantitative PCR

From livers and small intestinal segments, mRNA was isolated using TRI reagent (Sigma). Subsequently, cDNA was synthesized by a reverse transcription procedure using Moloney murine leukemia virus transcriptase and random primers according to manufacturer's protocol. mRNA expression levels were analyzed by means of real-time PCR, amplifying cDNA using appropriate primers and probes. PCR results of the liver and intestine were normalized to 18S mRNA levels. The sequences of the primers and probes of *18S*, short heterodimer partner (*Shp*), cholesterol 7 $\alpha$ -hydroxylase (*Cyp7A1*), sterol 12 $\alpha$ -hydroxylase (*Cyp8B1*), sterol 27-hydroxylase (*Cyp27A1*), *rev-erba* (*Rev-Erba*), ileal bile acid-binding protein (*Ibabp*), apical sodium-dependent bile salt transporter (*Asbt*), Na<sup>+</sup>-taurocholate co-transporting polypeptide (*Ntcp*), multidrug resistance-associated protein 2/3 (*Mrp2/3*), bile salt export pump (*Bsep*) and ATP binding cassette g5/g8 (*Abcg5/g8*) have been published (<http://www.LabPediatricsRug.nl>). For *Fgf15*, D site of albumin promoter (albumin D-box)-binding protein (*Dbp*), E4bp4 (*E4bp4*), *Fgfr4* and  $\beta$ -Klotho ( $\beta$ -*Klotho*) the primers and probe sequences are listed in Supplementary Table S1.

## Gas Chromatography

To examine biliary bile acid composition, bile acids were converted to their methyl ester/trimethylsilyl derivatives.<sup>21</sup> Bile acid composition was subsequently determined by means of a capillary gas chromatography. The hydrophobicity index was calculated according to Heuman *et al.*<sup>22</sup>

## Isotope Dilution Technique

The isotope dilution technique has been described in detail by Hulzebos *et al.*<sup>21</sup> After administration of 300  $\mu$ g [<sup>2</sup>H<sub>4</sub>]-cholate, the enrichment, defined as the increase in M<sub>4</sub>-cholate/M<sub>0</sub>-cholate relative to baseline measurements, was expressed as the natural logarithm of atom percent excess (ln APE) value. By means of the linear decay curves, obtained by linear regression analysis of the decay of ln APE over time for the individual mice, the fractional turnover rate (FTR, fraction of pool lost per day), pool size ( $\mu$ mol/100 g BW) and synthesis rate ( $\mu$ mol/100 g BW/day, determined by multiplying pool size and FTR) of cholate were calculated. The calculation of pool size was performed by using the formula:  $(D \times b \times 100) / e^a - D$ . In this formula 'a' represents the intercept on the y axis of the regression lines of the individual mice, 'D' is the administered amount of label and 'b' is the isotopic purity.

## Statistical Analysis

Results are presented as means  $\pm$  s.d. Differences between the two groups were determined by the non-parametric Mann–Whitney *U*-test. The level of significance for all statistical analyses was set at  $P < 0.05$ . Analyses were performed using SPSS 16.0 for Windows software (SPSS, Chicago, IL, USA).

## RESULTS

### Characteristics of Chow-Fed Intestine-Selective Fxr Knockout Mice

The mRNA expression profiles of *Fxr* and *Fgf15* along the small intestine were analyzed by RT-PCR. As shown in Figure 1, *Fxr* mRNA expression was, as expected, highest in the distal small intestine of WT mice. *Fgf15* was mainly expressed in the distal ileum of WT mice, but its expression pattern did not entirely coincide with *Fxr* expression. The iFXR-KO mice showed a virtually complete absence in *Fxr* and a strong reduction (average reduction: 82%) in *Fgf15* expression along the intestine. Targets of FXR were analyzed in three intestinal segments (proximal, mid and distal) and were found to be expressed at lower levels in the small intestine of iFXR-KO mice, ie, *Ibabp* and *Ost-a* expression increase toward distal direction and in the terminal ileum were decreased 87 and 49% in iFXR-KO mice, respectively (data not shown). Ileal expression of *Asbt*, known to be not regulated by FXR in the mouse,<sup>4</sup> increases into distal direction without showing differences between both groups. *Shp*, an important target gene of FXR in liver, turned out to be expressed predominantly in the proximal part of the small intestine in both groups and no difference between iFXR-KO and control mice could be detected.

At 3 months of age, body and liver weights of iFXR-KO mice were significantly lower than those of WT littermates (Table 1), but liver to body weight ratios were not different between the groups. The observed differences in body and liver weights were consistent, ie, were observed at all ages from 4 to 28 weeks and remained upon feeding with specific diets (data not shown and Supplementary Table S2). Apart from a rather moderate TCA-induced increase, no differences were observed in plasma AST and ALT activities between iFXR-KO and control mice (Table 1 and Supplementary Table S2). In addition, no differences were observed in liver morphology between the groups (Figure 2). Table 1 furthermore shows that reduced body weight in iFXR-KO mice was not due to decreased food intake. Whole body FXR-deficient mice show elevated plasma lipid levels,<sup>3,4</sup> with high plasma (HDL) cholesterol and triglyceride levels. In contrast, we did not observe any significant differences in plasma or in hepatic lipid contents between chow-fed WT and iFXR-KO mice (Table 1).

### Time-Dependent Effects of Intestine-Selective Fxr-Deficiency on Hepatic *Cyp7A1* and Intestinal *Fgf15* Expression

Because of the well-known diurnal rhythm of hepatic *Cyp7A1* expression,<sup>3,13,23</sup> we examined the consequence of intestinal FXR deficiency on diurnal hepatic *Cyp7A1* expression at four distinct time points, ie, at 0100, 0700, 1300 and 1900 hours. No differences herein were observed between both sexes (male data not shown).

At the start of the dark period (1900 hours), hepatic *Cyp7A1* expression was highest in both groups, as expected (Figure 3). Only during the night period (1900–0700 hours), *Cyp7A1* expression was significantly higher in iFXR-KO mice compared with WT controls. Expression of *Cyp8B1*, essential for the formation of cholic acid, did not show a clear day-night variation and was not significantly affected in the iFXR-KO mice. Furthermore, no differences were observed in hepatic *Fxr* and *Shp* expression between both groups. Observing this time-dependent effect of iFXR-deficiency on *Cyp7A1* expression, we



questioned whether the absence of intestinal FXR and Fgf15 signalling acts through transcription factors (*Dbp*, *Rev-erba* and/or *E4bp4*) involved in the regulation of the circadian rhythmicity of *Cyp7A1* expression. Figure 3 demonstrates that these transcription factors indeed showed a distinct circadian pattern in their expression profile, however, expression patterns were highly similar in both strains. Only *Dbp* and *Rev-erba* showed an increased expression in WT mice at a single time point (1900 hours), clearly not providing an explanation for the differences in *Cyp7A1* expression.

Exploring the circadian rhythm of *Fgf15* expression (Figure 4) revealed a peak in *Fgf15* expression at 0700 hours. As Fgf15 represses *Cyp7A1* expression, the expression profile of intestinal *Fgf15* turned out, as expected, to be exactly the reverse to hepatic *Cyp7A1* expression. Interestingly, no day–night variation in the expression of *Ibabp*, a well-established FXR target gene, was found in WT mice. *Fgf15* and *Ibabp* expression were significantly lower in the intestine-selective FXR knockout mice when compared with controls.

### Effect of Intestine-Selective Deletion of FXR on Bile Formation and Kinetics of the Enterohepatic Circulation of Bile Acids

As shown in Figure 5a, bile flow was significantly higher in iFXR-KO mice compared with controls. Biliary bile acid, cholesterol and phospholipid concentrations were not significantly different between the groups (data not shown). However, as a consequence of the higher bile flow rate, biliary bile acid and phospholipid output rates were significantly higher in the iFXR-KO mice than in controls. To assess the metabolic basis of altered bile formation, kinetic parameters of the enterohepatic circulation were determined upon intravenous injection of [<sup>2</sup>H<sub>4</sub>]-cholate. Figure 6a shows the cholate enrichments in plasma over time. From these regression curves, cholate pool size, FTR and synthesis rate were calculated. Cholate pool size of WT mice was ~ 40% smaller than that of iFXR-KO mice. However, the FTR was not significantly different between the groups. Cholate synthesis rate was calculated by multiplying cholic acid pool size and cholate FTR. Owing to a tendency toward a decreased FTR in iFXR-KO mice, the cholate synthesis rate did not reach a statistical significant difference between both groups. However, total bile acid synthesis as deduced from the fecal loss of bile acids, which equals the hepatic bile acid synthesis rate, was significantly higher in the iFXR-KO mice than in littermate controls (15.0 ± 1.0 μmol/day/100 g BW and 23.6 ± 2.5 μmol/day/100 g BW, WT and iFXR-KO mice, respectively).

Table 2 shows that, in addition to altered bile formation, the bile acid composition in bile was affected by intestinal FXR deficiency as well. In bile of iFXR-KO mice, an increased relative contribution of cholic acid and deoxycholic acid was observed, whereas β- and ω-muricholic acids, derived from chenodeoxycholic acid, were present at lower levels in bile of these mice. As a consequence of this compositional change, the mean hydrophobicity index of the bile acids in bile was increased in iFXR-KO mice when compared with WT controls.

Supplementary Figure S1 shows no differences in hepatic expression of genes involved in either hepatic FXR or Fgf15 signalling (*Fxr*, *Shp* and *Fgfr4*, *βKlotho*, respectively), bile acid synthesis (*Cyp27A1*, chenodeoxycholic acid formation) or hepatobiliary transport (*Ntcp*

(also known as *Slc10a1*, basolateral uptake of bile acids), *Mrp2* and *3* (also known as *Abcc2* and *3*, biliary anion secretion), *Bsep* (also known as *Abcb11*, biliary bile acid secretion) and *Abcg5/8* (biliary cholesterol secretion)) were observed.

### Effects of Bile Acid Feeding and Bile Acid Sequestration on Bile Formation and Bile Acid Synthesis in Intestine-Selective FXR-KO Mice

Feeding intestine-selective FXR-KO and WT mice a moderately bile acid-enriched diet (TCA; 0.5% w/w for 3 days) was used to increase the circulating bile acid pool. Figure 5 shows that, upon feeding this diet, bile flow tended to increase in both groups. The biliary bile acid, cholesterol and phospholipid output rates were all significantly increased upon TCA feeding. Interestingly, the differences between the two groups observed upon chow feeding were largely diminished in this condition. At the gene expression level, TCA-enriched diet feeding did not change the expression level of intestinal *Fxr*; however, caused a massive upregulation in *Shp* (> 30-fold) and *Fgf15* (> 30-fold) expression in the terminal ileum of control mice. In the liver, there was a relatively small increase in *Shp* expression, exclusively in iFXR-KO mice. Yet, Figure 7 shows a clear downregulation of *Cyp7A1* and *Cyp8B1* expression in control as well as in iFXR-KO mice, although the downregulation of *Cyp7A1* did not reach statistical significance in WT mice.

Sequestration of bile acids in the intestinal tract by means of a Colesevelam HCl-enriched diet reduced bile flow as well as in biliary bile acid, cholesterol and phospholipids output rates (Figure 5). Significant differences in cholesterol and phospholipids output rates between WT and iFXR-KO mice were observed despite similar bile acid output rates. However, these differences between the two groups were small when compared with the differences observed upon chow feeding. Bile acid sequestration did not change intestinal *Shp* expression, however, caused a steep decrease in *Fgf15* expression. Likely as a consequence hereof, we observed an upregulation in hepatic *Cyp7A1* expression in WT mice. Despite the already low expression of *Fgf15* in the iFXR-KO mice, we, surprisingly, observed a similar induction of hepatic *Cyp7A1* expression in iFXR-KO mice as in WT controls. *Cyp8B1* increased in both strains as well, although this did not reach statistical significance in the WT controls. Hepatic *Shp* expression did not change in iFXR-KO mice, however, was decreased in WT controls, possibly contributing to the observed increases in *Cyp7A1* and *Cyp8B1* expression.

## DISCUSSION

Bile acids exert important physiological functions in control of bile formation, cholesterol homeostasis and fat absorption. In addition, they also exert regulatory roles in triglyceride and glucose metabolism.<sup>1</sup> Maintaining bile acid homeostasis is therefore of great physiological relevance. The bile acid-activated FXR is an important factor in control of bile acid homeostasis. In addition to the established direct hepatic FXR pathway of *Cyp7A1* suppression, an indirect intestinal FXR-mediated signalling pathway has been identified.<sup>12,13</sup> Activation of intestinal FXR increases the expression of *Fgf15*. *Fgf15* travels through the circulation to the liver, where it represses *Cyp7A1*. The relative importance of direct control by hepatic FXR and indirect FXR-*Fgf15*-mediated control has remained elusive.



Recently, Kim *et al.*<sup>16</sup> addressed this issue by comparing intestine- and liver-selective FXR-KO mice. These authors concluded that repression of *Cyp7A1* was more strongly affected by disruption of intestinal FXR, whereas repression of *Cyp8B1* was more sensitive to loss of hepatic FXR.<sup>16</sup> This and earlier work<sup>24</sup> led to the general assumption that the intestinal FXR-Fgf15 pathway provides a major contribution to control of hepatic bile acid synthesis. Yet, the scientific evidence supporting this assumption is merely based on rather modest differences at the gene expression level. In contrast to Kim *et al.*,<sup>16</sup> we now focussed on the physiological consequences of intestinal FXR deficiency by assessing the effects on diurnal variation of the bile acid synthesis machinery, on the kinetics of bile acid metabolism and on the bile formation process. We showed that the effect of disrupting intestinal FXR on hepatic *Cyp7A1* expression is dependent on the time of the day, with less efficient suppression during the night phase when *Fgf15* expression is high in WT mice. The consequences are an increased bile flow and biliary secretion rates of bile acids and phospholipids. By means of a mouse-adapted isotope dilution technique,<sup>21</sup> we showed that the cholic acid pool size is significantly increased in the intestine-selective FXR knockout mice without differences in FTR. Increasing the circulating bile acid pool by means of TCA-enriched diet feeding and withdrawal of bile acids from the pool by sequestration minimized the observed differences between both strains.

We observed a consistent slight decrease in body weight of iFXR-KO mice (~ 15%), not mentioned by Kim *et al.*<sup>16</sup> As no differences in food intake or fecal energy content were found (data not shown), this likely reflects alterations in energy expenditure in iFXR-KO mice. This unexpected consequence of iFXR deficiency is currently under investigation.

It is well known that hepatic *Cyp7A1* expression displays a pronounced diurnal rhythm.<sup>3,13,23</sup> *Cyp7A1* expression turned out to be exclusively increased in iFXR-KO mice during the active night period, when *Fgf15* expression is high in WT mice. As no differences between both groups were observed for hepatic *Fxr* and *Shp* expression, we attribute this increase of *Cyp7A1* in iFXR-KO mice to low intestinal *Fgf15* expression in these mice, which is the direct consequence of the lack of intestinal FXR as confirmed by the examination of intestinal *Ibabp* expression. We conclude that intestinal FXR through Fgf15 controls hepatic bile acid synthesis mainly during the night period, which is in agreement with Houten *et al.*<sup>25</sup> who showed that intestinal FXR is most active during the night period by means of a transgenic FXR luciferase reporter mouse.<sup>25</sup>

Despite the time-dependent effect on *Cyp7A1* expression, iFXR-KO mice display an overall increased cholic acid pool size. As a consequence, biliary bile acid secretion was increased which, in turn, led to an increased bile flow and phospholipid output. This is in agreement with results from Yu *et al.*<sup>26</sup> These authors reported that *Fgfr4-deficient* mice, thus lacking hepatic Fgf15 signalling, also display an increased bile acid pool size and a higher rate of hepatobiliary bile acid secretion than their controls.

Upon feeding a moderate bile acid-enriched diet, biliary bile acid secretion was increased in both groups, associated with an increased phospholipids and cholesterol secretion. As intestinal FXR is disrupted in iFXR-KO mice, we did not expect to observe a decrease in hepatic *Cyp7A1* expression in these mice. However, increasing the bile acid pool led to a

downregulation of *Cyp7A1*, not reaching statistical significance in WT mice, and of *Cyp8B1* in both genotypes. The small increase in ileal *Fgf15* expression in combination with the increase in hepatic *Shp* expression might explain the observed decrease in *Cyp7A1* expression in the iFXR-KO mice. More importantly, most of the differences between the two strains observed in bile formation were minimized, implying that a rather moderate increase in bile acid flux through the liver (+ 30%) overrules the regulatory role of intestinal *Fgf15*.

Upon sequestration of bile acids in the intestinal tract, biliary bile acid secretion decreased in both groups, leading to decreased bile flow and phospholipids and cholesterol secretion. In accordance with TCA-enriched diet feeding, most of the observed differences between the two strains in the chow-fed condition were minimized. At the gene expression level, bile acid sequestration caused a decrease in intestinal *Fgf15* expression resulting in increased hepatic *Cyp7A1* and *Cyp8B1* mRNA levels. However, in WT mice we cannot exclude the contribution of decreased hepatic *Shp* expression.

Kim *et al*<sup>16</sup> concluded that intestinal FXR through *Fgf15* primarily regulates the expression of *Cyp7A1*, whereas *Cyp8B1* repression was more sensitive to loss of hepatic FXR.<sup>16</sup> However, the combination of their and our results indicates that some care is required in interpretation of these findings. In our study, 0.5% TCA-enriched diet feeding did not affect hepatic FXR signalling in WT mice, as evidenced by an unchanged hepatic *Shp* expression. However, this diet substantially decreased *Cyp8B1* at the gene expression level. In return, the sequestration of bile acids caused a significant decrease in hepatic FXR signalling in WT mice, as evident from a decreased hepatic *Shp* expression, without any difference in *Cyp8B1* mRNA levels. According to the conclusion of Kim *et al*,<sup>16</sup> hepatic *Cyp8B1* expression should not change upon disruption of intestinal FXR. In our present study, we indeed do not observe differences in *Cyp8B1* expression level between both strains; however, we did observe a difference in the relative biliary bile acid composition with a shift toward a more hydrophobic bile acid pool (hydrophobicity index -0.352 and -0.217 in WT and iFXR-KO mice, respectively) due to an increased contribution of hydrophobic bile acids species, such as cholic and deoxycholic acids, pointing to an increased contribution of *Cyp8B1* activity to hepatic bile acid synthesis.

Kim *et al*<sup>16</sup> do not explain why the iFXR-KO mice in their study did not display an increased basal *Cyp7A1* mRNA level. We show that this is most likely due to the time-dependent effect of deleting intestinal *Fgf15* on hepatic *Cyp7A1* expression. With respect to physiology, Kim *et al*<sup>16</sup> roughly estimated the bile acid pool size by extracting bile acids from freeze-dried liver, gallbladder and small intestine and showed that the total bile acid pool size tended to be increased in iFXR-KO mice compared with controls. By means of the microscale isotope dilution technique, we were able to show that iFXR-KO mice do display a significantly increased cholic acid pool size. This technique furthermore enabled us to examine the kinetic parameters of this bile acid pool: the increased cholic acid pool size appeared to be solely the consequence of an increased hepatic bile acid synthesis rate. A possible contribution of accelerated intestinal bile acid reabsorption could be excluded, as the calculated amount of cholate reabsorbed per day was not different between both strains (data not shown). Turnover and cycling of the bile acid pool occurred similarly in iFXR-KO and control mice, showing no differences in FTR, cycling frequency (pools/day) nor in

cycling time (h) (data not shown). As a consequence of the increased cholic acid pool size, biliary bile acid secretion was increased which, in turn, led to an increased bile flow and phospholipid output. In addition, we examined the contribution of intestinal FXR-Fgf15 signalling in control of hepatic bile acid synthesis and bile formation during modulation of the bile acid pool. We show that feeding a bile acid-containing diet or treatment with a bile acid sequestrant similarly affects bile formation in iFXR-KO and control mice and induced similar changes in *Cyp7A1* and *Cyp8B1* expression patterns.

From our present study we conclude that intestinal FXR-mediated Fgf15 production contributes to hepatic bile acid synthesis mainly during the dark period, when intestinal FXR activity is high. The disruption of intestinal FXR results in an increased cholic acid pool size leading to increased biliary bile acid secretion and therefore increased bile flow and phospholipids secretion. Modulation of the bile acid pool either by supplementation or sequestration of bile acids in the intestinal tract minimized the role of intestinal FXR-Fgf15 signalling present under normal dietary conditions.

## Supplementary Material

Refer to Web version on PubMed Central for supplementary material.

## ACKNOWLEDGEMENTS

We thank our colleagues for stimulating scientific discussions and advice. Our work is part of the project 'Hepatic and adipose tissue and functions in the metabolic syndrome' (HEPADIP, see <http://www.hepadip.org/>), which is supported by the European Commission as an Integrated Project under the 6th Framework Programme (Contract LSHM-CT-2005-018734). In addition, B.S. is recipient of a grant from 'Agence Nationale pour la Recherche' (ANR). Grant number: 'HEPADIP' (Contract LSHM-CT-2005-018734) and 'Agence Nationale pour la Recherche' (ANR).

## References

1. Russell DW. The enzymes, regulation, and genetics of bile acid synthesis. *Annu Rev Biochem* 2003;72:137–174. [PubMed: 12543708]
2. Cai SY, Boyer JL. FXR: a target for cholestatic syndromes? *Expert Opin Ther Targets* 2006;10:409–421. [PubMed: 16706681]
3. Kok T, Hulzebos CV, Wolters H, et al. Enterohepatic circulation of bile salts in farnesoid X receptor-deficient mice: efficient intestinal bile salt absorption in the absence of ileal bile acid-binding protein. *J Biol Chem* 2003;278:41930–41937. [PubMed: 12917447]
4. Sinal CJ, Tohkin M, Miyata M, et al. Targeted disruption of the nuclear receptor FXR/BAR impairs bile acid and lipid homeostasis. *Cell* 2000;102:731–744. [PubMed: 11030617]
5. Forman BM, Goode E, Chen J, et al. Identification of a nuclear receptor that is activated by farnesol metabolites. *Cell* 1995;81:687–693. [PubMed: 7774010]
6. Repa JJ, Mangelsdorf DJ. Nuclear receptor regulation of cholesterol and bile acid metabolism. *Curr Opin Biotechnol* 1999;10:557–563. [PubMed: 10600692]
7. Goodwin B, Jones SA, Price RR, et al. A regulatory cascade of the nuclear receptors FXR, SHP-1, and LRH-1 represses bile acid biosynthesis. *Mol Cell* 2000;6:517–526. [PubMed: 11030332]
8. Lu TT, Makishima M, Repa JJ, et al. Molecular basis for feedback regulation of bile acid synthesis by nuclear receptors. *Mol Cell* 2000;6:507–515. [PubMed: 11030331]
9. Duez H, Staels B. Rev-erbalph gives a time cue to metabolism. *FEBS Lett* 2008;582:19–25. [PubMed: 17765229]

10. Lavery DJ, Schibler U. Circadian transcription of the cholesterol 7 alpha hydroxylase gene may involve the liver-enriched bZIP protein DBP. *Genes Dev* 1993;7:1871–1884. [PubMed: 8405996]
11. Noshiro M, Usui E, Kawamoto T, et al. Multiple mechanisms regulate circadian expression of the gene for cholesterol 7alpha-hydroxylase (Cyp7a), a key enzyme in hepatic bile acid biosynthesis. *J Biol Rhythms* 2007;22:299–311. [PubMed: 17660447]
12. Inagaki T, Choi M, Moschetta A, et al. Fibroblast growth factor 15 functions as an enterohepatic signal to regulate bile acid homeostasis. *Cell Metab* 2005;2:217–225. [PubMed: 16213224]
13. Lundasen T, Galman C, Angelin B, et al. Circulating intestinal fibroblast growth factor 19 has a pronounced diurnal variation and modulates hepatic bile acid synthesis in man. *J Intern Med* 2006;260:530–536. [PubMed: 17116003]
14. Goetz R, Beenken A, Ibrahim OA, et al. Molecular insights into the klotho-dependent, endocrine mode of action of fibroblast growth factor 19 subfamily members. *Mol Cell Biol* 2007;27:3417–3428. [PubMed: 17339340]
15. Wu X, Ge H, Gupte J, et al. Co-receptor requirements for fibroblast growth factor-19 signaling. *J Biol Chem* 2007;282:29069–29072. [PubMed: 17711860]
16. Kim I, Ahn SH, Inagaki T, et al. Differential regulation of bile acid homeostasis by the farnesoid X receptor in liver and intestine. *J Lipid Res* 2007;48:2664–2672. [PubMed: 17720959]
17. Madison BB, Dunbar L, Qiao XT, et al. Cis elements of the villin gene control expression in restricted domains of the vertical (crypt) and horizontal (duodenum, cecum) axes of the intestine. *J Biol Chem* 2002;277:33275–33283. [PubMed: 12065599]
18. Kuipers F, van Ree JM, Hofker MH, et al. Altered lipid metabolism in apolipoprotein E-deficient mice does not affect cholesterol balance across the liver. *Hepatology* 1996;24:241–247. [PubMed: 8707269]
19. Bligh EG, Dyer WJ. A rapid method of total lipid extraction and purification. *Can J Biochem Physiol* 1959;37:911–917. [PubMed: 13671378]
20. Mashige F, Imai K, Osuga T. A simple and sensitive assay of total serum bile acids. *Clin Chim Acta* 1976;70:79–86. [PubMed: 947625]
21. Hulzebos CV, Renfurm L, Bandsma RH, et al. Measurement of parameters of cholic acid kinetics in plasma using a microscale stable isotope dilution technique: application to rodents and humans. *J Lipid Res* 2001;42:1923–1929. [PubMed: 11714862]
22. Heuman DM. Quantitative estimation of the hydrophilic-hydrophobic balance of mixed bile salt solutions. *J Lipid Res* 1989;30:719–730. [PubMed: 2760545]
23. De Fabiani E, Mitro N, Gilardi F, et al. Coordinated control of cholesterol catabolism to bile acids and of gluconeogenesis via a novel mechanism of transcription regulation linked to the fasted-to-fed cycle. *J Biol Chem* 2003;278:39124–39132. [PubMed: 12865425]
24. Lefebvre P, Cariou B, Lien F, et al. Role of bile acids and bile acid receptors in metabolic regulation. *Physiol Rev* 2009;89: 147–191. [PubMed: 19126757]
25. Houten SM, Volle DH, Cummins CL, et al. *In vivo* imaging of farnesoid X receptor activity reveals the ileum as the primary bile acid signaling tissue. *Mol Endocrinol* 2007;21:1312–1323. [PubMed: 17426284]
26. Yu C, Wang F, Kan M, et al. Elevated cholesterol metabolism and bile acid synthesis in mice lacking membrane tyrosine kinase receptor FGFR4. *J Biol Chem* 2000;275:15482–15489. [PubMed: 10809780]

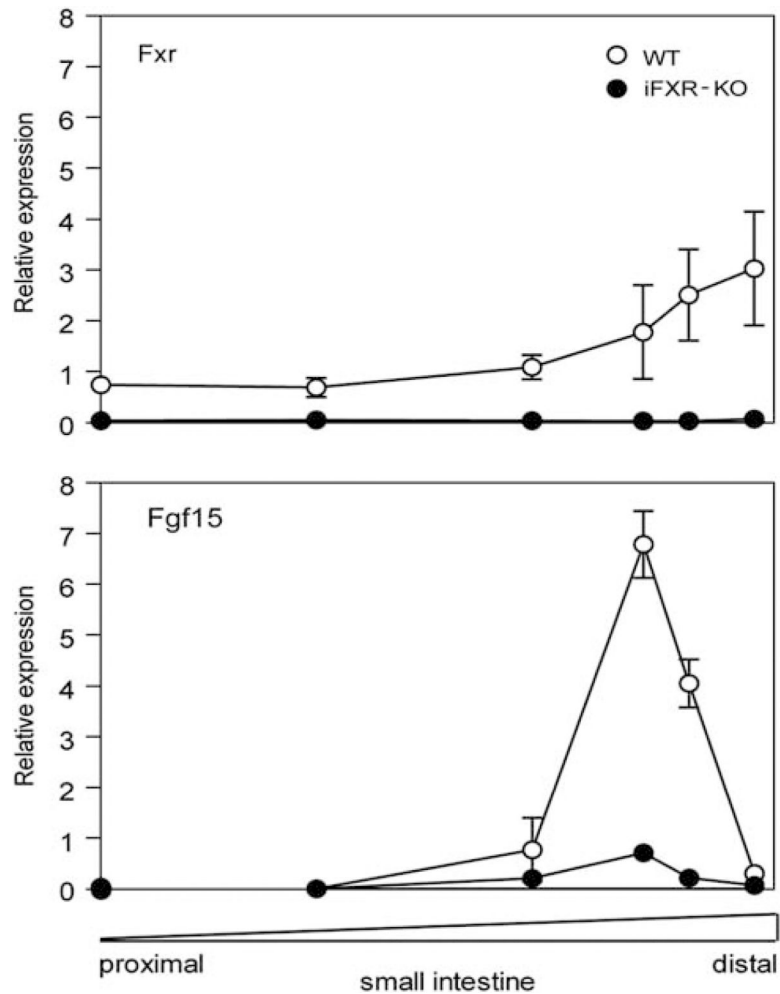


**Figure 1.** Relative gene expression pattern along the small Intestine. The small Intestine of male wild-type (WT) mice (open circles,  $n = 3$ ) and male intestine-selective FXR knockout mice (solid circles,  $n = 3$ ) was rinsed with PBS and six segments were excised; 0, 33, 66, 83, 90 and 100% (relative distance from stomach to distal ileum). Relative gene expression levels of *Fxr* and *Fgf15* compared with *18S* were analyzed using RT-PCR. Values are expressed as means  $\pm$  s.d.

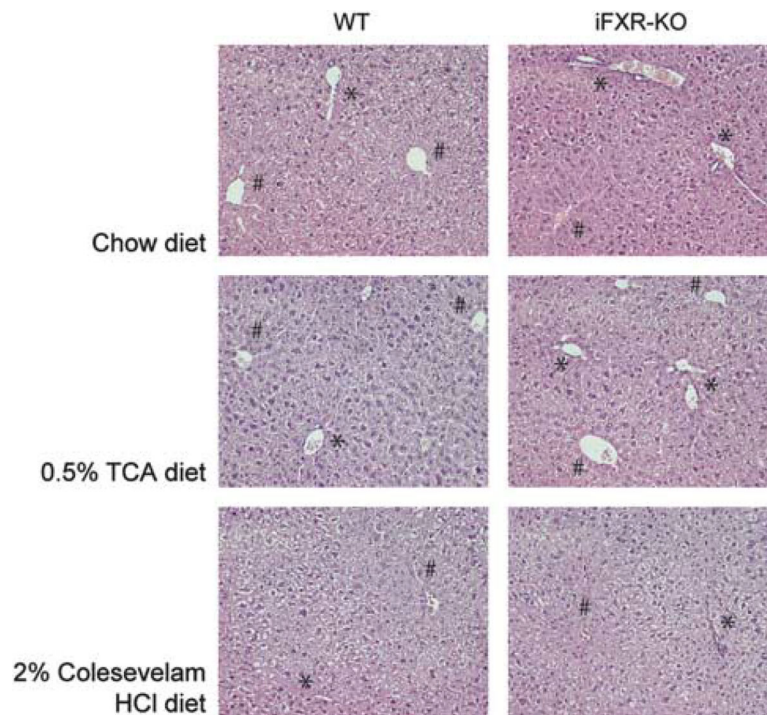


**Figure 2.** Liver morphology upon chow, 0.5% TCA- or 2% Colesevelam HCl-enriched diet feeding of WT and intestine-selective FXR knockout mice. Histological examination of liver morphology was assessed by hematoxylin/ eosin staining (see ‘Materials and Methods’ section). Liver morphology of WT and intestine-selective FXR knockout mice upon chow, 0.5% TCA- or 2% Colesevelam HCl-enriched diet feeding are represented at  $\times 20$  magnification. ‘\*’ Represents periportal hepatocytes; # represents pericentral hepatocytes.



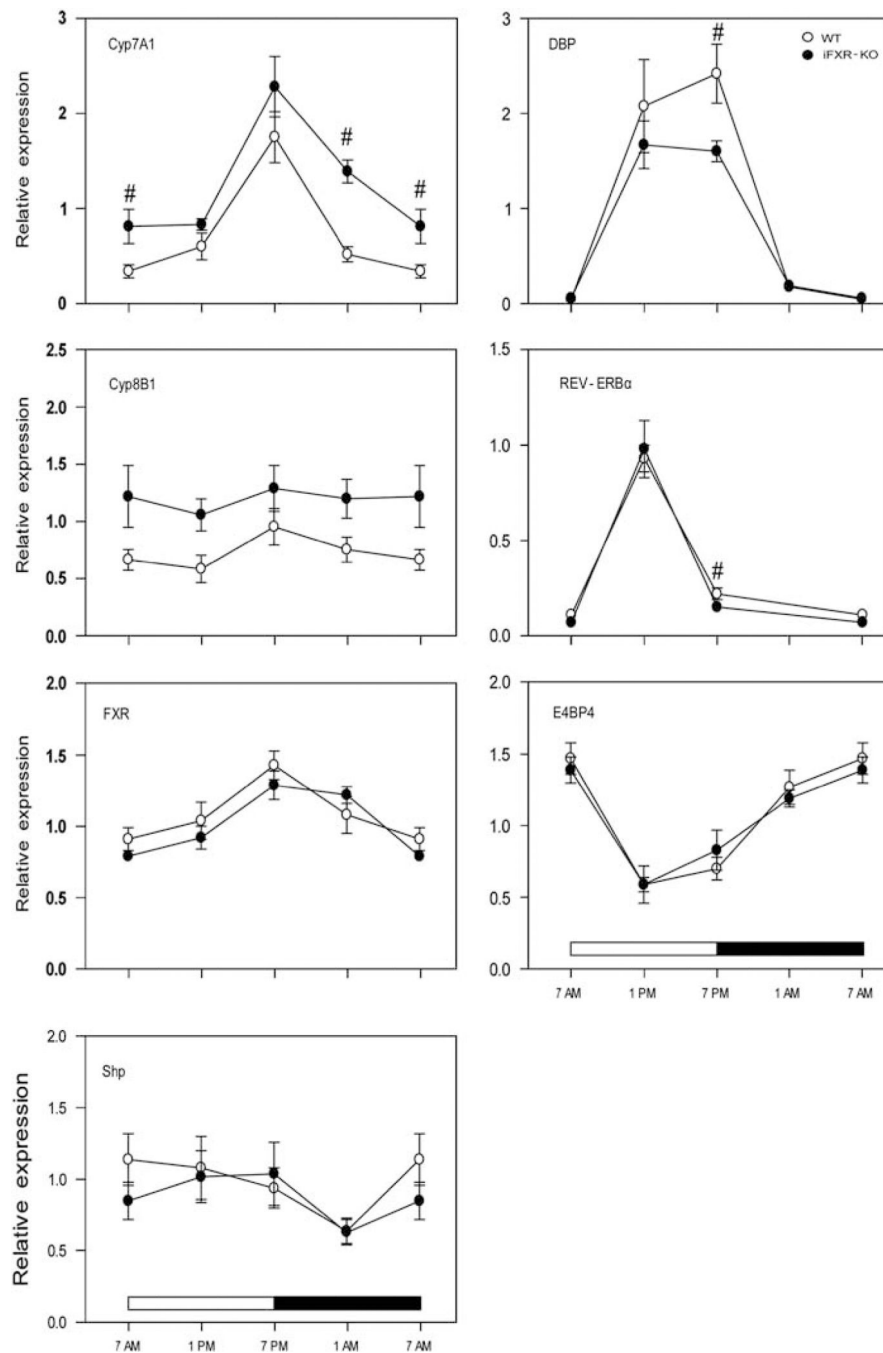


**Figure 3.** Circadian expression profile of genes involved in the regulation of hepatic bile acid synthesis. Gene expression levels (relative to *18S* expression) were measured at four time points (0700, 1300, 1900 and 0100 hours) in 6–7 female wild-type controls (open circles) or female intestine-selective FXR knockout mice (closed circles). Data are represented as mean  $\pm$  s.d. *Cyp7A1* and *Cyp8B1* are key enzymes in bile acid synthesis, *Shp* is the second messenger of FXR and *Dbp*, *Rev-erba* and *E4bp4* are involved in maintaining the circadian

rhythm of *Cyp7A1* expression. <sup>#</sup> Represents a significant difference with  $P < 0.05$  between the two analyzed strains.

Author Manuscript

Author Manuscript

Author Manuscript

Author Manuscript

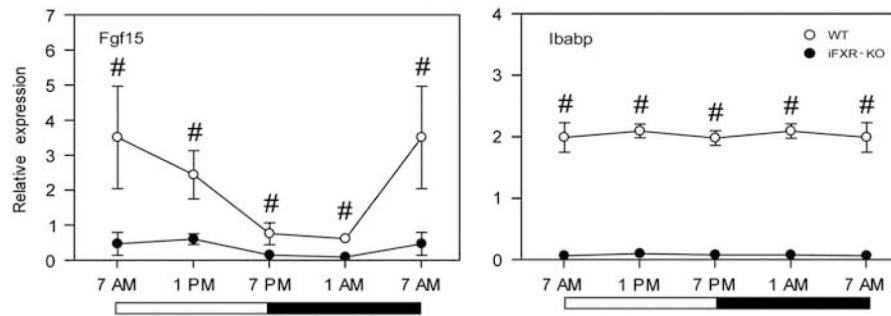


**Figure 4.**

Circadian expression profile of intestinal genes. Gene expression levels (relative to *18S*) were measured at four time points (0700, 1300, 1900 and 0100 hours) in ~4cm of terminal ileum proximal to the ileocecal sphincter either of female wild-type controls (open circles) or female intestine-selective FXR knockout mice (closed circles);  $N=4$ . Data are represented as mean $\pm$ s.d. *Fgf15* is the growth factor whose expression is induced by active intestinal FXR; *Ibabp*, ileal bile acid-binding protein, is an intestinal FXR target gene. '#' Represents a significant difference with  $P<0.05$  between the two analyzed strains.

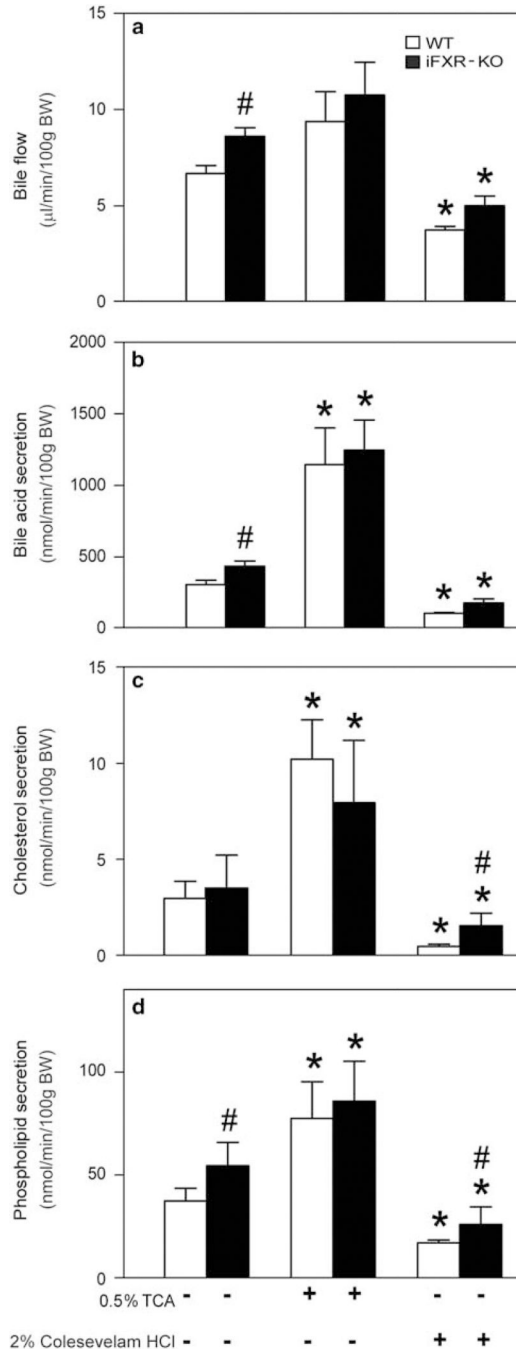


**Figure 5.** Bile flow (a) and biliary output rates (b–d) in wild-type (WT) and intestine-selective FXR knockout mice fed either a chow, 0.5% TCA- or 2% Colesevelam HCl-enriched diet. After 0.5% TCA-enriched diet or 2% Colesevelam HCl-enriched diet feeding for three respectively 7 days, mice ( $N=5$ ) were subjected to bile cannulation. As a result bile flow and biliary output rates were obtained. Open bars: WT littermates, closed bars: intestine-selective FXR knockout mice. Values are expressed as means  $\pm$  s.d. ‘#’ Represents a

statistical significance of  $P < 0.05$  between chow- and TCA-/Colesevelam HCl-fed mice. # is a statistical significance ( $P < 0.05$ ) between the two strain fed the same diet.

Author Manuscript

Author Manuscript

Author Manuscript

Author Manuscript

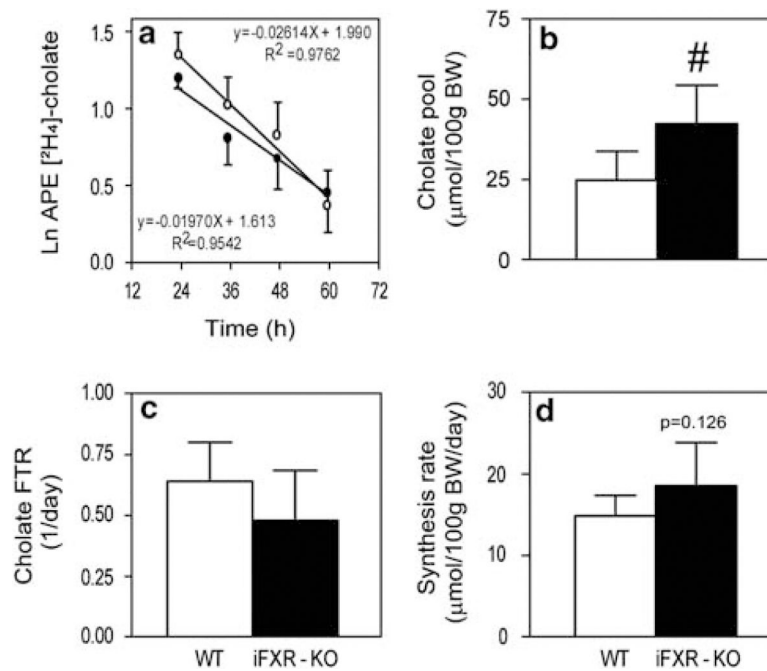


**Figure 6.**

Effects of intestine-selective FXR deficiency on decay of  $[\text{2H4}]$ -cholate (a), pool size (b), fractional turnover rate (c) and cholate synthesis rate (d). Mice were subjected to bile cannulation, as described in experimental procedures section. (a–d) are derived from the  $[\text{2H4}]$ -cholate isotope enrichment measurements in plasma of wild-type (WT) and intestine-selective FXR knockout mice.  $N=6$  per strain: WT mice (open bars) and intestine-selective FXR knockout mice (closed bars). Data are represented as means $\pm$ s.d. # significant difference ( $P < 0.05$ ) between the WT and intestine-selective FXR knockout (iFXR-KO) mice.



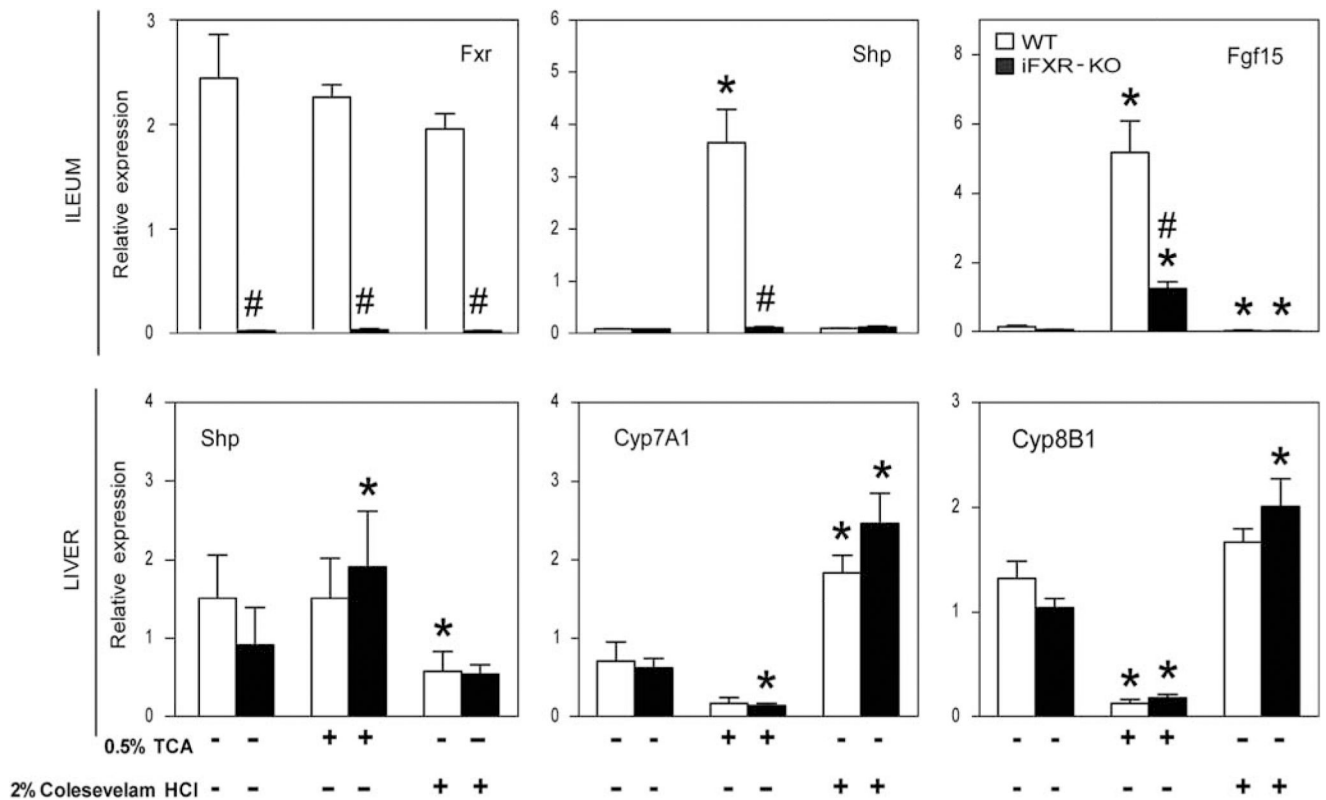


**Figure 7.**

Relative gene expression of wild-type (WT) and intestine-selective FXR knockout mice fed either a chow, 0.5% TCA- or 2% Colesevelam HCl-enriched diet. Quantitative real-time PCR was performed on ~ 1.5 cm of terminal ileum proximal to the ileocecal sphincter as well as on liver tissue (expressed as relative expression compared with *18S*). Total RNA of WT (open bars) and intestine-selective FXR knockout mice (closed bars) fed either a standard chow or a 0.5% TCA- or 2% Colesevelam HCl-enriched diet (samples taken between 0930 and 1300 hours). Data are represented as means  $\pm$  s.d. '\*' Represents a significant difference of  $P < 0.05$  within a strain when compared with the chow-fed condition. #  $P < 0.05$ , WT vs intestine-selective FXR knockout mice.

**Table 1**

Animal characteristics of chow-fed wild-type and intestine-selective FXR knockout mice

|                                     | Chow diet     |                          |
|-------------------------------------|---------------|--------------------------|
|                                     | WT            | iFXR-KO                  |
| Body weight (g)                     | 35.7 ± 2.86   | 30.5 ± 2.56 <sup>#</sup> |
| Liver weight (g)                    | 1.95 ± 0.24   | 1.69 ± 0.09 <sup>#</sup> |
| Ratio LW/BW                         | 0.054 ± 0.003 | 0.056 ± 0.003            |
| Food intake (g/24h)                 | 5.24 ± 0.26   | 5.13 ± 0.35              |
| Feces production (g/24h)            | 1.01 ± 0.08   | 0.99 ± 0.02              |
| <i>Plasma lipids (mM)</i>           |               |                          |
| Triglycerides                       | 0.98 ± 0.56   | 0.77 ± 0.31              |
| Total cholesterol                   | 2.50 ± 0.61   | 2.24 ± 0.36              |
| Free cholesterol                    | 1.05 ± 0.35   | 0.95 ± 0.22              |
| Cholesteryl esters                  | 1.45 ± 0.29   | 1.29 ± 0.19              |
| Free fatty acids                    | 0.44 ± 0.12   | 0.46 ± 0.14              |
| <i>Plasma liver enzymes (U/l)</i>   |               |                          |
| AST                                 | 112 ± 19      | 115 ± 28                 |
| ALT                                 | 28 ± 7        | 22 ± 7                   |
| Liver proteins (mg/g liver)         | 188.2 ± 13.2  | 185.0 ± 14.0             |
| <i>Liver lipids (nmol/mg liver)</i> |               |                          |
| Triglycerides                       | 13.12 ± 7.59  | 10.49 ± 5.80             |
| Total cholesterol                   | 8.57 ± 4.17   | 8.82 ± 4.39              |
| Free cholesterol                    | 7.62 ± 3.53   | 7.87 ± 3.68              |
| Cholesteryl esters                  | 0.94 ± 0.67   | 0.95 ± 0.75              |
| Phospholipids                       | 30.19 ± 6.66  | 30.65 ± 5.70             |

Samples are taken in the fed condition at 1300 hours. LW, liver weight; BW, body weight. Values are expressed as means ± s.d. (N = 6).

<sup>#</sup> P < 0.05 vs control.

**Table 2**

Bile acid profile in bile of chow-fed wild-type and intestine-selective FXR knockout mice

|                               | Chow diet      |                             |
|-------------------------------|----------------|-----------------------------|
|                               | WT             | iFXR-KO                     |
| Total biliary bile salts (mM) | 27.55 ± 3.80   | 29.58 ± 7.22                |
| <i>Bile salt species (%)</i>  |                |                             |
| Chenodeoxycholate             | 0.93 ± 0.36    | 1.02 ± 0.51                 |
| Cholate                       | 47.10 ± 8.14   | 62.70 ± 7.05 <sup>#</sup>   |
| Deoxycholate                  | 1.96 ± 1.11    | 3.32 ± 0.73 <sup>#</sup>    |
| Hyodeoxycholate               | 0.75 ± 0.11    | 0.83 ± 0.14                 |
| $\alpha$ -Muricholate         | 3.46 ± 0.64    | 3.13 ± 1.39                 |
| $\beta$ -Muricholate          | 41.94 ± 9.13   | 26.15 ± 6.13 <sup>#</sup>   |
| $\omega$ -Muricholate         | 2.02 ± 0.26    | 1.06 ± 0.23 <sup>#</sup>    |
| Ursodeoxycholate              | 1.84 ± 0.23    | 1.78 ± 0.31                 |
| Hydrophobicity index          | -0.352 ± 0.073 | -0.217 ± 0.054 <sup>#</sup> |

Groups are composed of six chow-fed male mice and samples were taken around 1300 hours. Values are expressed as means ± s.d.

<sup>#</sup> $P < 0.05$  vs control.

Author Manuscript

Author Manuscript

Author Manuscript

Author Manuscript